NUCL SCI TECH (2017) 28:8
DOI 10.1007/s41365-016-0158-7

Geant4 simulation of $^{238}U(n,f)$ reaction induced by D-T neutron source

Chang-Lin Lan[1,2] · Meng Peng[1] · Yi Zhang[1] · Zheng Wei[1] · Ze-En Yao[1,2] · Bao-Lin Xie[1]

Received: 28 April 2016 / Revised: 13 July 2016 / Accepted: 24 July 2016 / Published online: 1 December 2016

Abstract Knowledge of actinides (n,f) fission process induced by neutron is of importance in the field of nuclear power and nuclear engineering, especially for reactor applications. In this work, fission characteristics of $^{238}U(n,f)$ reaction induced by D-T neutron source were simulated with Geant4 code from multiple perspectives, including the fission production yields, total nubar, kinetic energy distribution, fission neutron spectrum and cumulative γ-ray spectrum of the fission products. The simulation results agree well with the experimental nuclear reaction data (EXFOR) and evaluated nuclear data (ENDF). Mainly, this work was to examine the rationality of the parametric nuclear fission model in Geant4 and to direct our future experimental measurements for the cumulative fission yields of $^{238}U(n,f)$ reaction.

Keywords Fission characteristics · Geant4 code · $^{238}U(n,f)$ reaction · D-T neutron source · Decayed γ-ray spectrum

This work is supported by the National Natural Science Foundation of China (No. 21327801).

✉ Chang-Lin Lan
lanchanglin2000@163.com

1 School of Nuclear Science and Technology, Lanzhou University, Lanzhou 730000, China

2 Key Laboratory of Special Function Materials and Structure Design, Ministry of Education, Lanzhou 730000, China

1 Introduction

Fission characteristics of actinides induced by neutrons are important for reactor applications. In particular, the neutron-induced fission data of ^{235}U, ^{238}U and ^{239}Pu has a significant application in conventional light-water reactors, heavy-water reactors and fast reactors [1, 2]. Among the three actinides, ^{238}U is associated with ^{235}U in conventional reactor and correlate with ^{239}Pu in fast reactor. The knowledge of $^{238}U(n,f)$ fission reaction induced by neutron at around 14 MeV produced by a D-T neutron source has a wide range of applications, such as accelerator-driven subcritical systems [3–6], thorium-based molten-salt reactors [7], nuclear transmutation system [8], fission reaction rate measurement [9] and nuclear structure research. For these applications, detailed information of the fission cross section, fission-fragment mass, kinetic energy distributions, fission neutron spectrum and γ-ray spectrum is key observables. So far, the measured FPY (Fission Product Yield) for ^{238}U (n,f) reaction induced by neutrons mainly came from early experiment in low-energy region. The investigation of their dependence on production rates of secondary long-lived fission residues and neutron-rich isotopes may not only reveal valuable information about the shape of the nuclear potential energy landscape around the saddle point, but also provide reliable fission data for further experimental study and the nuclear facility design.

The FPY of ^{238}U changes with the neutron spectrum and flux, irradiation time, etc. The methods to measure the fission products include radiochemistry, mass spectrometry, direct γ-spectroscopy [10, 11], line isotope separation, etc. Now, it is possible to simulate nuclear reaction process with a Monte Carlo transport code—Geant4 version 9.6.4 (GEometry And Tracking code) [12, 13]. As a new tool for simulating the ^{238}U fission reaction induced by D-T neutron source, Geant4 has been used in high-energy physics, space, medical, nuclear experiments and accelerator physics [14, 15]. In a simulation, necessary particles and physical processes were constructed to set up the physics framework. For fission processes of ^{238}U, the G4NeutronHPElastic model, G4NeutronHPInelastic model, G4Decay model, G4NeutronHPCapture model and G4ParaFissionModel model were specifically selected to describe the elastic scattering, inelastic scattering, decay process, neutron capture and neutron-induced fission, respectively.

Many authors have reported their researches on the characteristic of FPY distribution for ^{238}U(n,f) reaction induced by neutron [11, 16–26], and evaluation databases [27], such as ENDF/B-VII.1, JEFF/FPY-2011, JENDL-4.0, and GEFY-3.3, are available. However, many provided just segmental fission nuclides or fission yield distribution. In this paper, typical simulation results are compared with experimental data [28] and evaluation data to evaluate the physics model in Geant4, in an attempt to understand characteristic of ^{238}U(n,f) fission reaction, and guide our future measurements for the cumulative fission yields of ^{238}U(n,f) reaction induced by D-T neutrons using the direct γ-spectroscopy method.

2 Simulations

2.1 The incident neutron spectrum

Fast neutron generators are used worldwide for all kinds of purposes, such as nuclear data measurement, radiation hardening and radioactive breeding, etc. The neutrons from D-T neutron generator are suitable for inducing fission reactions research. Lanzhou University has developed an intense neutron generator based on T(d,n)^{4}He reaction with a rotating target, to generate 14.0 MeV monoenergetic neutrons by 300 keV deuteron beams from an accelerator. The fast neutrons produced with a thick target have distinct angular distribution and intrinsic energy spectrum [29]. For an incident deuteron energy E_d, the neutron spectrum with a given angle θ and energy E can be calculated by Eq. (1) [30]:

$$\frac{d^2Y}{dE_n d\Omega_n} = N \int_0^{E_0} \left[\frac{d^2\sigma}{dE_n d\Omega_n}\right]_{(E_d,\theta_n)} \left[\frac{dE_d}{dx}\right]^{-1} \times \exp\left(-\int_{E_d}^{E_0} \sum\nolimits_{non}(E') \left[\frac{dE_d}{dx}\right]^{-1} dE'\right) dE_d, \quad (1)$$

where $d^2Y/(dE_n d\Omega_n)$ is the double differential thick target neutron yields, N is atomic number density of the target, $d^2\sigma/(dE_n d\Omega_n)$ is the neutron-produced double differential cross section, E_0 is the incident deuteron energy, E_d is the deuteron energy in the target, dE_d/dx is the stopping power of the target and $\sum_{non}(E')$ is the macroscopic total reaction cross section. In this work, we calculated the neutron spectrum with incident deuteron beams of 260 keV, as shown in Fig. 1.

2.2 Sample

Uranium dioxide (100.0% purity) was used as the target. In order to determine optimum thickness of the ^{238}U sample, we chose ^{128}Te and ^{92}Zr as representative nuclides to calculate the different share of fission fragments deposition, as function of the sample thickness. As shown in Fig. 2, the deposition share reaches more than 99.90% at 0.8 mm thickness, where it begins changing slowly with the thickness. Therefore, 1.0 mm target thickness (over 99.95% fragments deposition share in the sample) was selected.

A hollow cylindrical target of Φ20 mm in wall thickness of 1.0 mm was used in the simulation. The target was positioned on the deuteron beam axis. Fission products identified in each step of nuclear reaction inside the sample were considered in Geant4, whereas fission neutrons and decay γ-rays were recorded in the entire 4π steradian.

3 Results and discussion

3.1 Fission yields distribution

The FPY distribution is a key to fission reaction. In the ^{238}U(n,f) fission process, the fission fragments were

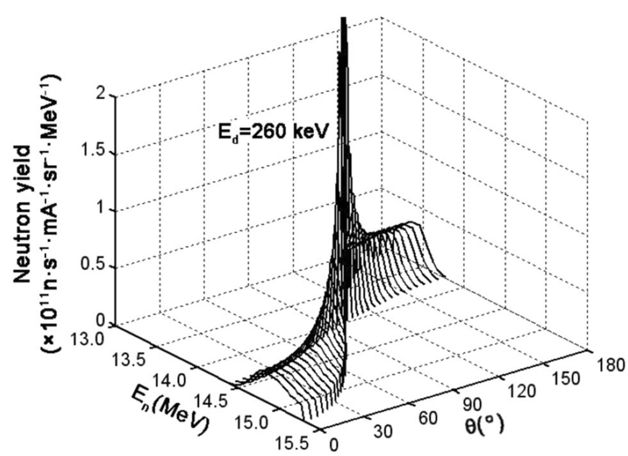

Fig. 1 Outgoing neutron energy spectrum distribution of D-T neutron source

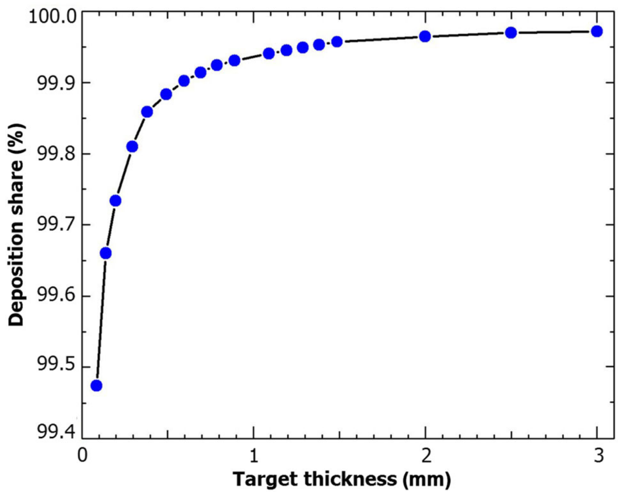

Fig. 2 Simulated deposition share of the fission-fragments, as function of target thickness

simulated in their independent and cumulative yields. The former considered the initial fission-fragment yields only, while the latter took all the fission products including the initial fragments and the β-decayed nuclides from the excited state of fission-fragments.

The independent FPY yields vs. Z and N is shown in Fig. 3. The fission fragments spread over upper left of the β-stability line in charge number $Z = 35–55$ and neutron number $N = 60–85$, then decay to the bottom of the stability ground state.

The simulated independent FPY distribution was compared with the nuclear data from ENDF/B-VII.I library. As shown in Fig. 4, they agree well with each other. According to the nuclear fission theory, the pre-neutron emission mass distribution of neutron-induced antinides can be treated as symmetrical fission which obeys to certain specific rules. As a result, the heavy and light fission-

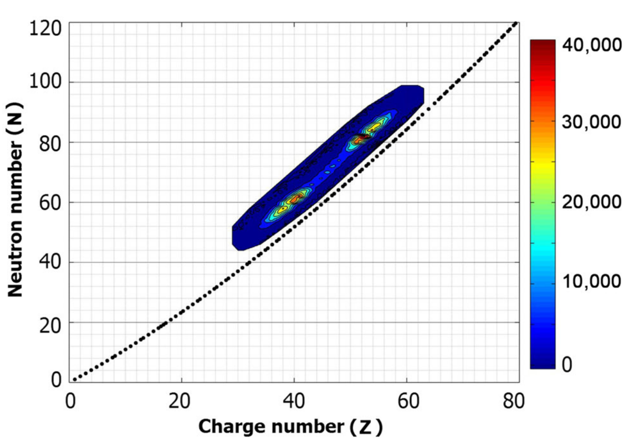

Fig. 3 Independent yields distribution of the ^{238}U(n,f) fission reaction induced by D-T neutrons. The *color scale* refers to the number of events

fragment masses have their own symmetrical peak. The heavy mass peak in fragment mass distributions is roughly constant and close to $A_2 = 140$, and the complementary light mass peak in fragment mass distributions can be calculated by $A_1 = A_f - A_2$, where A_f is the fission nucleus mass number. There is a deep valley in symmetrical fission-fragment mass distribution center position $A_0 = A_f/2$. From our simulation, the heavy mass peak in fragment mass distributions is at $A_2 = 137$, corresponding to the five-dimensional energy landscapes model [31], which gives a less deviation (<5%) than the phenomenological fission potential model [32] that assumes $A_2 = 140$ for the mass number of heavy fragment.

In Fig. 5, the calculated cumulative FPY distributions for isobaric chain are compared with the experimental data from EXFOR and the evaluated data from ENDF/B-VII.1. In Fig. 5a, the calculated results agree well with the evaluated data, but are higher than the experimental data within error bars. In Fig. 5b, the three data sets are of good consistency in a wide range, but for $A < 75$ and $A > 160$, our calculation results are lower than the evaluated data.

In the ^{238}U(n, f) reaction induced by 14 MeV neutrons, the yields of light fission fragment around mass number of 94 and the heavy fission fragment around mass number 140 are found to be higher because of the nuclear structure effects and suitable N/Z values. Meanwhile, the FPY distribution does not have a third peak around symmetric mass region, due to the lower excitation energy of ^{238}U(n,f) reaction induced by 14 MeV neutrons, leading to asymmetric fission of fission-fragment with mass number. So, the physical models in Geant4 code are suitable for simulating the neutron-induced fission process for actinide nuclide.

3.2 Fission-fragment kinetic energy distribution

In the fission reaction process of ^{238}U induced by fast neutrons, the ^{238}U nucleus splits into two fission fragments with high kinetic energies. They separate and fly away under the action of Coulomb repulsion. Figure 6 shows the relationship between the kinetic energy and mass number of the fission fragments. The nuclides with magic number of nucleons are much more than other fission fragments. The primary kinetic energy of each heavy fission fragment is in the order of 50–110 MeV, which means that the primary fission fragments can be in velocities of 10^7 m/s, before they slow down via elastic-scattering inside the uranium sample. The huge kinetic energy of fission fragment transforms into the thermal energy or emits a light particle to ground state in de-excitation process and releases its kinetic energy in elastic-scattering process, which is important for reactor design especially in selecting reactor materials.

Figure 7 shows the average and total fission-fragment kinetic energies as function of the mass number. According

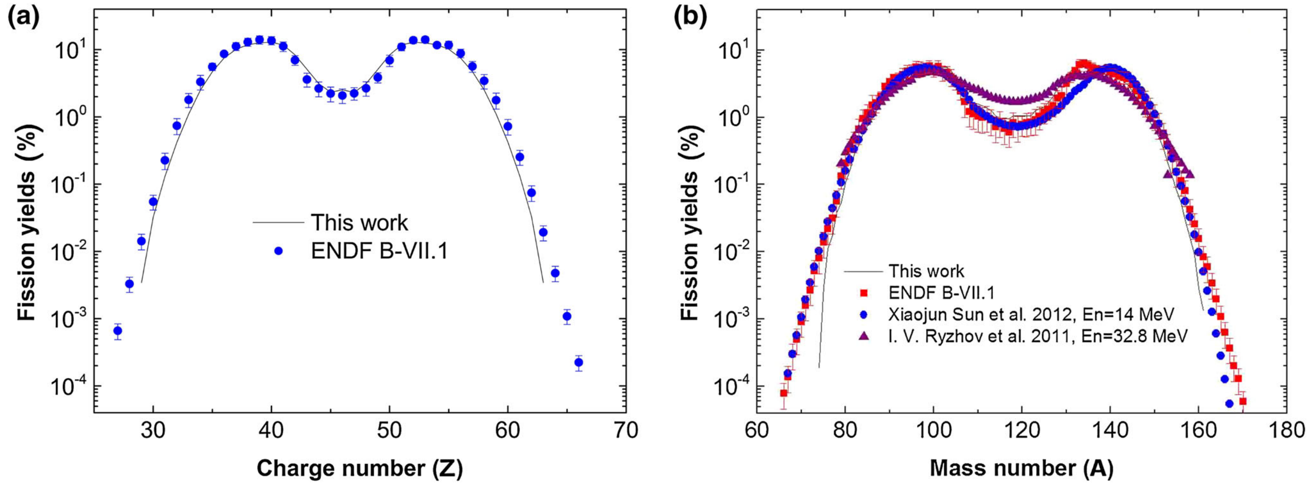

Fig. 4 Comparison of independent FPY from ^{238}U (n, f) reaction between the calculated and recommended data. **a** The elemental yield versus charge number. **b** The mass chain yield versus mass number

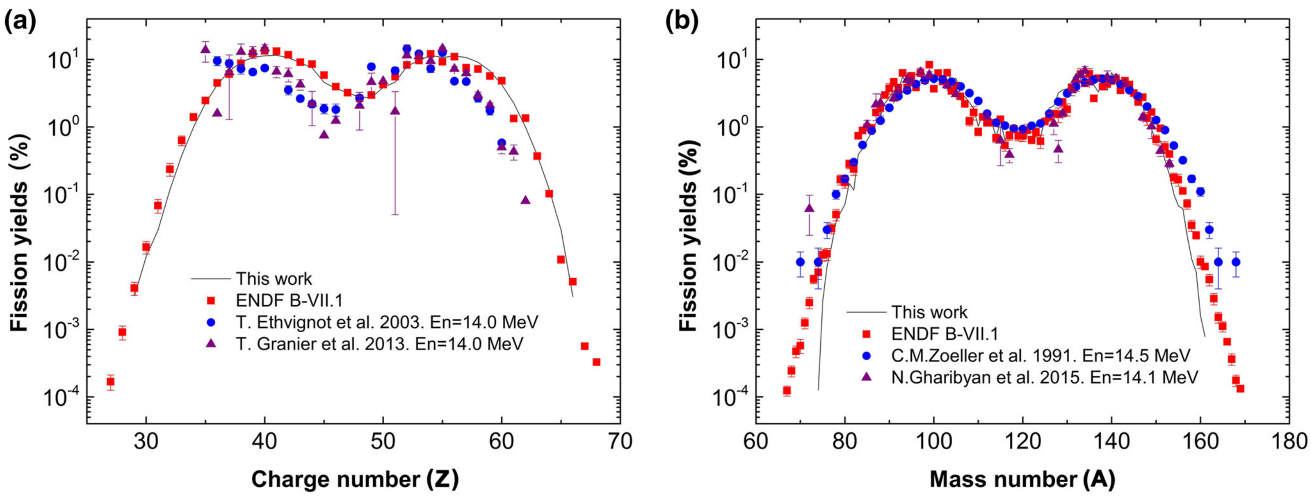

Fig. 5 Calculated FPY of ^{238}U (n,f) reaction as function of the charge number (**a**) and mass number (**b**), compared with the recommended data

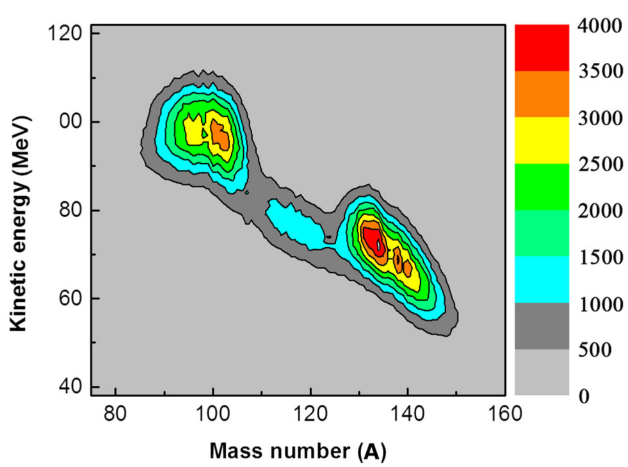

Fig. 6 Primary FPY kinetic energy distribution from ^{238}U(n,f) reaction induced by D-T neutrons. The *color scale* refers to the number of events

to the momentum conservation law, the light fission-fragments have higher kinetic energy and the heavy ones have lower kinetic energy. The total kinetic energy is the sum of kinetic energies of a complementary fragment pair. From Fig. 7b, the total kinetic energy of heavy fission-fragment reaches to the maximum value at mass number of 132 due to the nuclear shell structure effects. The structure of fission fragment with mass number of 132 ($Z = 50$, $A = 82$) approximates that a sphere that helps to minimize the center-to-center distance of two fission fragments contributes to bigger fission fragment kinetic energy.

3.3 Fission neutron spectrum

The fission neutron spectrum, including prompt and delayed neutrons, is of importance in basic research and reactor design. The prompt neutrons are mainly evaporated

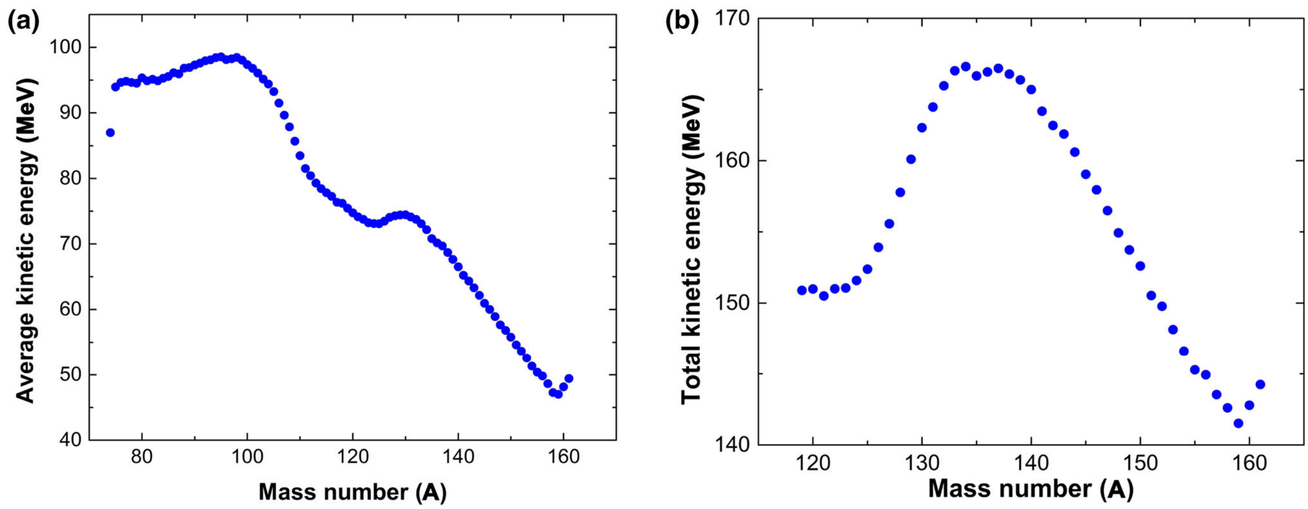

Fig. 7 Relationship between the fission-fragment kinetic energy distribution and the fission-fragment mass number. **a** The average kinetic energy distribution. **b** The total kinetic energy distribution

by the primary neutron-rich fission fragments far from the β-stability line, with high excited energy. They account for over 99% of the total fission neutrons. The delayed neutrons are produced from fission fragments within β-decay. Figure 8 shows the neutron spectrum from the ^{238}U(n,f) reaction induced by D-T neutrons.

The total fission neutron energy distribution obeys Maxwell–Boltzmann distribution, which can be calculated by:

$$f(E) = n_0 (E/\pi)^{1/2} (kT)^{-3/2} e^{-E/(kT)}, \tag{2}$$

where $f(E)$ is the fission neutron energy spectrum, E is the neuron energy, parameter $kT = 1.38$ is the Maxwell temperature and $n_0 = 2.11 \times 10^{-6}$ is the proportional coefficient of the function.

We also calculated the total nubar (the average fission neutron count) of ^{238}U(n,f) reaction at different energies of the incident neutron beams. The results are compared with experimental data in Ref. [33] (Fig. 9). The average fission neutron count (ν) changes mainly with the cross section of ^{238}U(n,f) reaction, in a positive correlation with incident neutron energy. The excitation energy of ^{238}U fission system increases with the incident neutron energy as more neutrons are evaporated immediately in the order of 10^{-15}s.

3.4 Decay γ-ray spectrum of ^{238}U (n, f) reaction

In the neutron-induced fission reaction, the residual nucleus emits characteristic γ-ray in its de-excitation process, and can be thus identified by analyzing the decay γ-ray spectrum. The cumulative γ-ray spectra of fission

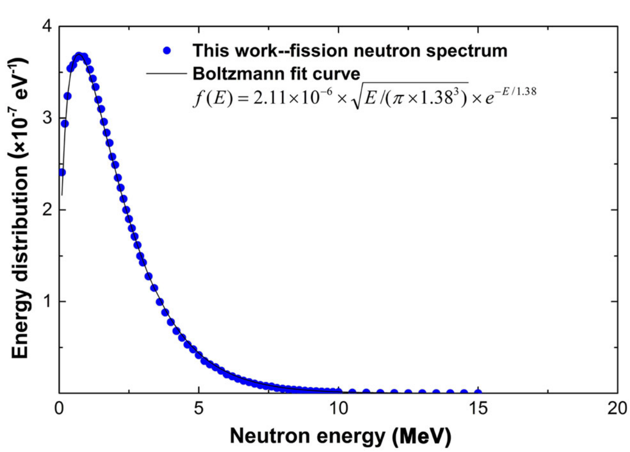

Fig. 8 Fission neutron spectrum of ^{238}U(n,f) reaction induced by D-T neutrons

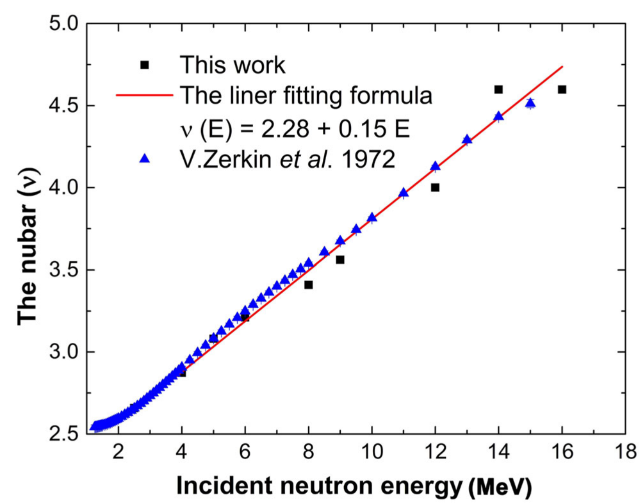

Fig. 9 Total nubar of ^{238}U (n,f) reaction as function of the incident neutron energy

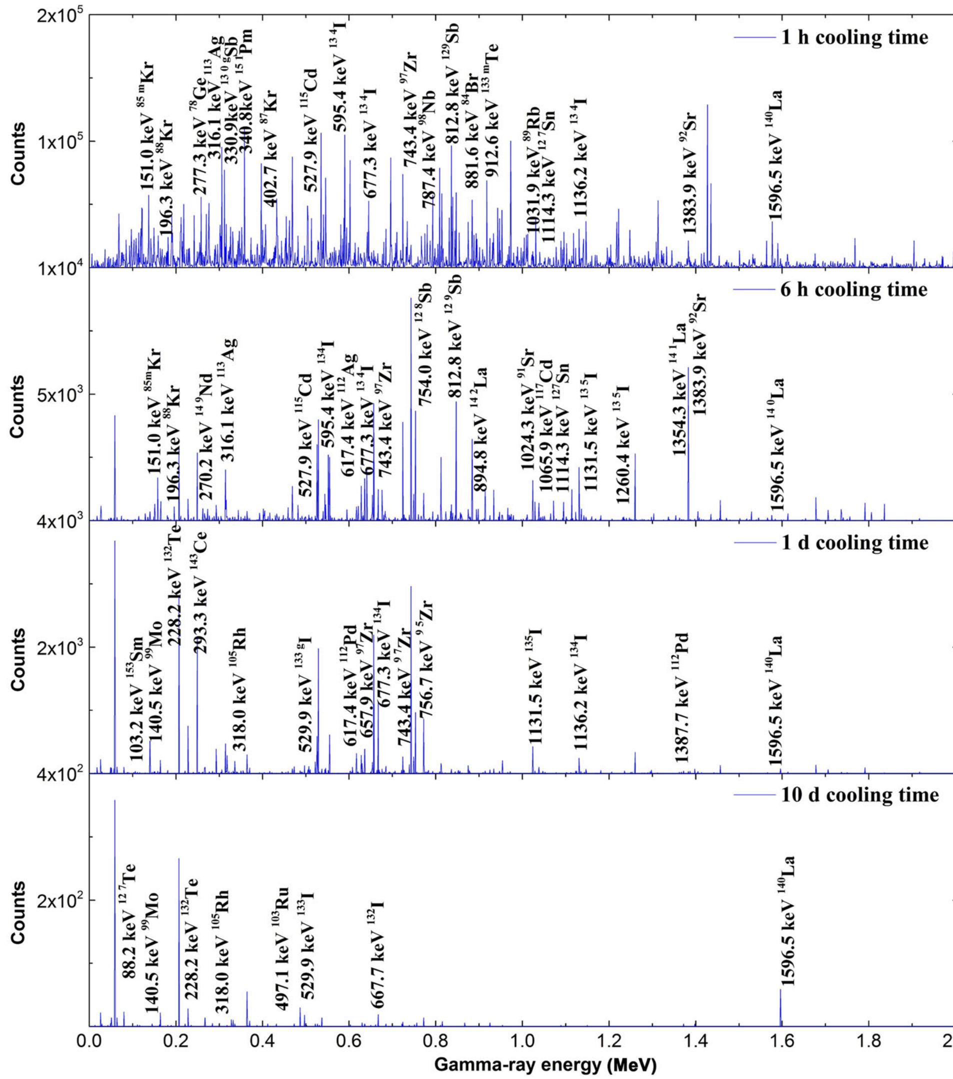

Fig. 10 Cumulative γ-ray spectrum from ^{238}U fission reaction with different cooling time

products from ^{238}U(n,f) reaction induced by D-T neutron source, of different cooling times, are shown in Fig. 10.

The precise fission-fragment γ-ray data of fission productions [34] for analyzing fission yield is partly presented in Table 1. It is possible to distinguish over 34 fission products (Fig. 10) of different half-lives using correlative calculation process [35]. This is helpful for our future experimental measurements for the cumulative fission yields of ^{238}U(n,f) reaction.

4 Conclusion

The characteristics of ^{238}U(n,f) reaction induced by neutron around 14 MeV have been investigated using the Monte Carlo program Geant4 for the first time. The fission production yields distribution, fission-fragments kinetic energy distribution, total nubar, fission neutron spectrum and decayed γ-ray spectrum were represented and discussion. Meanwhile, the calculated values of independent yield and cumulative FPY distribution were compared with the obtainable experimental and evaluation data. The calculation results indicate that the Geant4 code with the parametric nuclear fission model is scientific rationality and able to predict the following experimental measurement of ^{238}U(n,f) reaction.

1. The calculated results of independent yield and cumulative FPY distribution versus the charge and mass number are in good agreement with the datum from EXFOR and ENDF/B-VII.1, which indicates that the Geant4 code with the fission model can simulate ^{238}U(n,f) reaction induced by D-T fast neutron precisely. The calculated result is useful for our experimental measurement preparation.
2. The computational result of fission-fragment kinetic energy distribution conforms to the momentum conservation law. The kinetic energy of fission-fragment

Table 1 Characteristic γ-ray of partly fission nuclide for fission reaction of ^{238}U(n,f)

Nuclides	Half-life	γ-Ray energy (keV)	γ-Ray intensity (%)	Nuclides	Half-life	γ-Ray energy (keV)	γ-Ray intensity (%)
^{78}Ge	1.45 h	277.3	96.0	^{127g}Sn	2.10 h	1095.6	19.0
^{84}Br	31.8 min	881.6	41.6			1114.3	38.0
^{85m}Kr	4.48 h	151.0	75.2	^{128g}Sb	9.01 h	754.0	100.0
		304.5	14.0	^{129}Sb	4.32 h	812.8	43.5
^{87}Kr	76.3 min	402.7	49.7	^{130g}Sb	40.0 min	330.9	78.0
^{88}Kr	2.84 h	196.3	26.3	^{132}I	2.30 h	522.7	16.7
		834.8	13.1			667.7	13.9
^{89}Rb	15.4 min	1031.9	63.6	^{132}Te	78.2 h	228.2	88.1
^{91}Sr	9.48 h	652.9	11.1	^{133m}Te	55.4 min	647.4	15.6
		749.8	23.0			912.6	45.8
		1024.3	32.5	^{133g}I	20.8 h	529.9	87.0
^{92}Sr	2.71 h	1383.9	90.0	^{134}I	52.6 min	595.4	11.1
^{95}Zr	64.02 d	756.7	55.4			677.3	7.8
^{97}Zr	16.7 h	743.4	92.7			1136.2	9.2
^{98}Nb	53.4 min	787.4	93.4	^{135}I	6.61 h	1131.5	22.5
^{99}Mo	66 h	140.5	5.70			1260.4	28.6
^{103}Ru	39.3 d	497.1	90.9	^{140}La	40.2 h	1596.5	95.5
^{105}Rh	35.4 h	318.9	19.2	^{141}La	3.93 h	1354.3	2.63
^{112}Pd	21.1 h	617.4	49.9	^{142}La	1.55 h	641.2	53.0
		1387.7	6.24			894.8	9.40
^{112}Ag	3.13 h	617.5	13.0	^{143}Ce	33.0 h	293.3	43.4
^{113}Ag	5.37 h	316.1	1.29	^{149}Nd	1.728 h	211.3	27.3
^{115g}Cd	53.5 h	527.9	27.5			270.2	10.7
^{117m}Cd	3.40 h	1065.9	23.1	^{151}Pm	53.08 h	340.8	23.0
^{127m}Te	9.35 h	88.2	0.086	^{153}Sm	46.28 h	103.2	30.0

with magic nucleus is higher with the nuclear shell effect. The fission neutron spectrum obeys the Boltzmann distribution.

3. The cumulative γ-ray spectrum can be used to identify the kinds and yields of fission products with the characteristic energy and intensity of γ-ray. It will direct us to acquire the information of FPY in following experimental measurement.

All of the above, the fission physical models in Geant4 provide us a new way to calculate the fission process, analyze the experimental data and extend the nuclear evaluation data as well as reactor engineering design. It lays a good foundation for measure the cross sections and fission yields from ^{238}U(n,f) reaction with direct γ-spectroscopy method.

References

1. T.R. Allen, D.C. Crawford, Lead-cooled fast reactor systems and the fuels and materials challenges. Sci. Technol. Nucl. Install, 2007, Article ID 97486. DOI:10.1155/2007/97486
2. J. Krepel, S. Pelloni, K. Mikityuk, Comparison of open and closed U–Pu equilibrium fuel cycles for Generation-IV fast reactors with the EQL3D procedure. Nucl. Eng. Des. **250**, 392–402 (2012). doi:10.1016/j.nucengdes.2012.06.004
3. X. Cao, Z.X. He, C.R. Qing et al., Feasibility study of ^{233}U production with accelerator driven sub-critical system (in Chinese). Sci. Sin.-Phys. Mech. Astron. **42**, 437–444 (2012). doi:10.1360/132012-205
4. Nuclear Energy Agency Organization for Economic Co-operation and Development. Accelerator-driven Systems (ADS) and Fast Reactors (FR) in Advanced Nuclear Fuel Cycles. http://www.oecd-nea.org/ndd/reports/2002/nea3109-ads.pdf
5. The European Technical Working Group on ADS (2001). A European roadmap for developing accelerator driven systems (ADS) for nuclear waste incineration. http://www.oecd-nea.org/pt/docs/ADS%20ROADMAP.pdf
6. H. Nifenecker, S. David, J.M. Loiseaux et al., Basics of accelerator driven subcritical reactors. Nucl. Instrum. Methods A **463**(3), 428–467 (2001). doi:10.1016/S0168-9002(01)00160-7
7. J.J.L. Yoonjo, P.S. Matthew, C.K. John et al., Thorium fuel cycle for a molten salt reactor: State of Missouri feasibility study. 121st ASEE Annual Conference & Exposition, Indianapolis, IN (2014). DOI: 10.13140/RG.2.1.2828.6803
8. Transmutation of radioactive waste. http://www.oecd-nea.org/trw/
9. X.X. Chen, Z.D. Fan, Y. Wang et al., Experimental research of ^{238}U fission reaction rate in China Experimental Fast Reactor. Atom. Energy Sci. Technol. **47**, 120–122 (2013). doi:10.7538/yzk.2013.47.so.0120. **(in Chinese)**

10. W.M.D. Jesse, Gamma-ray spectroscopy by direct crystal diffraction. Annu. Rev. Nucl. Sci **8**, 163–180 (1958). doi:10.1146/annurev.ns.08.120158.001115
11. T. Granier, R.O. Nelson, T. Ethvignot et al., Measurement of prompt X-rays in ^{238}U (n, f) from threshold to 400 MeV. Eur. Phys. J. A **49**, 114 (2013). doi:10.1140/epja/i2013-13114-8
12. CERN (2013) Geant4 Installation Guide: Building and installing Geant4 for users and developers. http://geant4.web.cern.ch/geant4/UserDocumentation/UsersGuides/InstallationGuide/fo/BookInstalGuide.pdf
13. Physics Reference Manual (2012) http://geant4.web.cern.ch/geant4/UserDocumentation/UsersGuides/PhysicsReferenceManual/BackupVersions/V9.6/fo/PhysicsReferenceManual.pdf
14. X. Qin, R. Zhou, J.F. Han et al., GEANT4 simulation of the characteristic gamma-ray spectrum of TNT under soil induced by DT Neutrons. Nucl. Sci. Tech. **26**(1), 42–47 (2015). doi:10.13538/j.1001-8042/nst.26.010501
15. Z. Wei, Z.E. Yao, C.L. Lan et al., Monte Carlo simulation of fission yields, kinetic energy, fission neutron spectrum and decay γ-ray spectrum for 232Th(n, f) reaction induced by 3H(d, n)4He neutron source. J. Radioanal. Nucl. Chem. **305**(2), 455–462 (2015). doi:10.1007/s10967-014-3910-7
16. D.J. Gorman, R.H. Tomlinson, Cumulative yields in the 14-MeV neutron fission of ^{238}U. Can. J. Chem. **46**, 1663–1672 (1968)
17. L.H. Gevaert, R.E. Jerv, H.D. Sharma, Cumulative yields in the 14 MeV neutron fission of ^{232}Th and ^{238}U in the symmetric region. Can. J. Chem. **48**, 641–651 (1970)
18. W.X. Li, T.Y. Sun, X.H. Sun, et al. Charge distribution in the fission of ^{238}U by 14.7 MeV neutron. Nucl. Chem. Radiochem. **2**, 9–16. (in Chinese)
19. C. Chung, M.Y. Woo, Fission product yields in the fast-neutron fission of ^{238}U. J. Radioanal. Nucl. Chem. **109**, 117–131 (1987)
20. N. Gharibyan, K.J. Moody, J.D. Despotopulos, First fission yield measurements at the National Ignition Facility: 14-MeV neutron fission of ^{238}U. J. Radioanal. Nucl. Chem. **303**(2), 1335–1338 (2014). doi:10.1007/s10967-014-3474-6
21. E. Dobreva, N. Nenoff, Yields of fission products with masses A = 131 to 135 for the fast neutron induced fission of U-238. J. Radioanal. Nucl. Chem. **81**(1), 29–36 (1984)
22. H. Naik, S. Mukerji, R. Crasta et al., Measurement of fission product yields in the quasi-mono-energetic neutron-induced fission of ^{238}U. Nucl. Phys. A **941**, 16–37 (2015). doi:10.1016/j.nuclphysa.2015.05.006
23. J. Laurec, A. Adam, T. de et al., Fission product yields of ^{233}U, ^{235}U, ^{238}U and ^{239}Pu in fields of thermal neutrons, fission neutrons and 14.7-MeV neutrons. Nucl. Data Sheets **111**, 2965–2980 (2010). doi:10.1016/j.nds.2010.11.004
24. H.D. Selby, M.R. Mac Innes, D.W. Barr et al., Fission product data measured at Los Alamos for fission spectrum and thermal neutrons on ^{239}Pu, ^{235}U, ^{238}U. Nucl. Data Sheets **111**, 2891–2922 (2010). doi:10.1016/j.nds.2010.11.002
25. M. Mac Innes, M.B. Chadwick, T. Kawano. Fission product yields for 14 MeV neutrons on ^{235}U, ^{238}U and ^{239}Pu. Nucl. Data Sheets **112**, 3135–3152 (2011). doi:10.1016/j.nds.2011.11.009
26. T. Ethvignot, T. Granier, P. Casoli, et al. Experimental studies of prompt neutron and photon emission in intermediate energy neutron-induced fission, Fission & Properties of Neutron-rich Nuclei, 2003:418-425. DOI: 10.1142/9789812705211_0060
27. ENDF: Evaluated Nuclear Data File. https://www-nds.iaea.org/exfor/endf.htm
28. IAEA-EXFOR Database. https://www-nds.iaea.org/exfor/exfor.htm
29. Z.E. Yao, W.M. Yue, P. Luo et al., Neutron yield, energy spectrum and angular distribution of accelerator-based T(d, n) ^{4}He reaction neutron source for thick target. Atom. Energy Sci. Technol **42**(5), 400–403 (2008)
30. K. Hirabayashi, T. Nishizawa, H. Uehara, Measurement of neutron yields from thick Al and SUS304 targets bombarded by 5-MeV and 9-MeV deuterons. Prog. Nucl. Sci. Technol. **3**, 60–64 (2012)
31. P. Moller, D.G. Madland, A.J. Sierk et al., Nuclear fission modes and fragment mass asymmetries in a five-dimensional deformation space. Nature **409**(6822), 785–790 (2001). doi:10.1038/35057204
32. X.J. Sun, C.G. Yu, N. Wang, Pre-neutron-emission mass distributions for low-energy neutron-induced actinide fission. Phys. Rev. C **85**, 014613 (2012). doi:10.1103/PhysRevC.85.014613
33. F. Manero, V.A. Konshin, Status of the energy dependent nu-values for the heavy isotopes (Z > 90) from thermal to 15 MeV and nu-values for spontaneous fission. At. Energy Rev **10**(4), 637–756 (1972)
34. Interactive chart of nuclides. http://www.nndc.bnl.gov/chart/
35. Z. Li, A.Z. Cui, D.M. Liu et al., Precise determination of yields of ^{95}Zr, ^{140}Ba and ^{147}Nd (in Chinese). J. Nucl. Radiochem. **17**(2), 65–72 (1995)